HHS Public Access

Author manuscript

J Vis Exp. Author manuscript; available in PMC 2023 August 09.

Integrated Photoacoustic, Ultrasound, and Angiographic Tomography (PAUSAT) for Non-invasive Whole Brain Imaging of Ischemic Stroke

Luca Menozzi[1,*], **Ángela del Águila**[2,*], **Tri Vu**[1], **Chenshuo Ma**[1], **Wei Yang**[2], **Junjie Yao**[1]

[1]Department of Biomedical Engineering, Duke University, Durham, NC, USA, 27708

[2]Multidisciplinary Brain Protection Program, Department of Anesthesiology, Duke University School of Medicine, Durham, NC, USA 27710

ABSTRACT:

An experimental ischemic stroke study using our newly developed non-invasive imaging system is presented that integrates three acoustic-based imaging technologies: photoacoustic, ultrasound, and angiographic tomography (PAUSAT). Combining these three modalities helps acquire multi-spectral PAT of brain blood oxygenation, high-frequency ultrasound imaging of the brain tissue, and acoustic angiography of the cerebral blood perfusion. The multi-modal imaging platform allowed the study of cerebral perfusion and oxygenation changes in the whole mouse brain after stroke. Two commonly used ischemic stroke models were evaluated: the permanent middle cerebral artery occlusion (pMCAO) model and the photothrombotic (PT) model. PAUSAT was used to image the same mouse brains before and after a stroke and quantitatively analyze both stroke models. This imaging system was able to clearly show the brain vascular changes after ischemic stroke, including significantly reduced blood perfusion and oxygenation in the stroke infarct region (ipsilateral) compared to the uninjured tissue (contralateral). The results were confirmed by both laser speckle contrast imaging and triphenyltetrazolium chloride (TTC) staining. Furthermore, stroke infarct volume in both stroke models was measured and validated by the TTC staining as the ground truth. Through this study, we have demonstrated that PAUSAT can be a powerful tool in non-invasive and longitudinal preclinical studies of ischemic stroke.

SUMMARY:

This work demonstrates the use of a multimodal ultrasound-based imaging platform for non-invasive imaging of ischemic stroke. This system allows for the quantification of blood oxygenation through photoacoustic imaging and impaired perfusion in the brain through acoustic angiography.

Corresponding authors: Wei Yang: wei.yang@duke.edu; Junjie Yao: junjie.yao@duke.edu.
*These authors contributed equally

A complete version of this article that includes the video component is available at http://dx.doi.org/10.3791/65319.

DISCLOSURES: The authors declare no conflict of interest in this work.

INTRODUCTION:

Blood transports oxygen (via the hemoglobin protein) and other important nutrients to the tissues in our bodies. When the flow of blood through tissues is interrupted (ischemia), severe damage to the tissues can occur, the most immediate effects of which are due to a lack of oxygen (hypoxia). Ischemic stroke is the result of interrupted blood flow to a certain region of the brain. The brain damage resulting from an ischemic stroke can occur within minutes of a vessel blockage, and can often have debilitating and lasting effects[1,2]. A highly valuable strategy to evaluate the physiopathology after ischemic stroke and identify and test new treatments is the use of small-animal models in the lab. Treatments discovered in the lab aim to be translated to clinical use and improve the patients' life. However, the use of animals in pre-clinical research needs to be carefully evaluated to fulfill the three R's rules: replacement, reduction, and refinement. The main purpose of this rule is to reduce the number of animals used in preclinical studies without risking valuable information. With this in mind, being able to longitudinally evaluate the lesion evolution while keeping the animal alive allows a great advantage in reducing the number of animals required as well as maximizing the information obtained from each animal[3].

Photoacoustic tomography (PAT) is a hybrid imaging modality that combines optical absorption contrast with ultrasound imaging spatial resolution[4]. The imaging mechanism of PAT is as follows: An excitation laser pulse is illuminated on the target being imaged. Assuming the target absorbs light at the wavelength of the excitation laser, it will increase in temperature. This quick increase in temperature results in a thermoelastic expansion of the target. The expansion causes an ultrasound wave to propagate out from the target. By detecting the ultrasound wave at many positions, the time required for the wave to propagate from the target to the detectors can be used to create an image, through a reconstruction algorithm. The ability of PAT to detect optical absorption in deep tissue regions differentiates PAT from ultrasound imaging, which detects boundaries of differing acoustic impedance of tissues[5]. In the visible and near-infrared spectra, the primary highly absorbing biomolecules that are abundant in organisms are hemoglobin, lipids, melanin, and water[6]. Of particular interest in the study of stroke is hemoglobin. Since oxyhemoglobin and deoxyhemoglobin have different optical absorption spectra, PAT can be used with multiple excitation laser wavelengths to determine the relative concentration of the two states of the protein. This allows the oxygen saturation of hemoglobin (sO_2), or blood oxygenation, to be quantified in and outside of the infarct region[7,8]. This is an important measure in ischemic stroke, as it can indicate the level of oxygen in the damaged brain tissue following ischemia.

Acoustic angiography (AA) is a contrast-enhanced ultrasound imaging method that is particularly useful for imaging the morphology of vasculature *in vivo*[9]. The method relies on the use of a dual-element wobbler transducer (a low frequency element and a high frequency element) in conjunction with microbubbles injected into the circulatory system of the imaging subject. The low-frequency element of the transducer is used for transmitting at the resonant frequency of the microbubbles (e.g., 2 MHz), while the high-frequency element is used to receive the superhamonic signals of the microbubbles (e.g., 30 MHz). When excited at a resonant frequency, the microbubbles have a strong nonlinear response, resulting in the production of super harmonic signals that surrounding body tissues do not produce[10].

By receiving with a high-frequency element, this ensures that only the microbubble signals are detected. Since the microbubbles are confined to the blood vessels, the result is an angiographic image of blood vessel morphology. AA is a powerful method for imaging ischemic stroke because the microbubbles that are flowing through the circulatory system will not be able to flow through blocked vessels. This allows AA to detect regions of the brain that are not perfused due to ischemic stroke, which indicates the infarct region.

Preclinical ischemic stroke research generally relies on the use of histology and behavioral testing to assess the location and severity of the stroke. Triphenyltetrazolium chloride (TTC) staining is a common histological analysis used to determine the stroke infarct volume. However, it can only be used at an endpoint, since it requires the animal to be euthanized[11]. Behavioral tests can be used to determine the motor function impairment at multiple timepoints, but they cannot provide quantitative anatomical or physiological values[12]. Biomedical imaging provides a more quantitative approach to studying the effects of ischemic stroke non-invasively and longitudinally[8,13,14]. However, existing imaging technologies can come at a high cost (such as small-animal magnetic resonance imaging [MRI]), be unable to provide concurrent structural and functional information, or have limited penetration depth (as most optical imaging techniques).

Here, we combine photoacoustic, ultrasound, and angiographic tomography (PAUSAT, see system diagram in Figure 1), which allows for complementary structural and functional information of blood perfusion and oxygenation following ischemic stroke[15]. These are two important aspects in assessing the severity of the injury and monitoring the recovery or response to treatments. Using these integrated imaging methods can increase the amount of information obtained by each animal, reducing the number of animals required and providing more information in the study of potential treatments for ischemic stroke.

PROTOCOL:

All animal procedures were approved by the Duke University Medical Center Animal Care and Use Committee and were conducted in accordance with the United States Public Health Service's Policy on Humane Care and Use of Laboratory Animals. Male and female C57BL/6J mice (see Table of Materials) were used for these studies. A minimum of 3 animals were imaged *per* stroke model group. See Figure 2 for the workflow followed in this protocol.

1. Inducing the stroke mouse model

1.1. Permanent middle cerebral artery occlusion (pMCAO) with common carotid artery (CCA) ligation.

NOTE: Briefly, perform permanent ligation of the right CCA and posterior electrocauterization of the right middle cerebral artery (MCA)[16]. This procedure limits the cerebral blood flow in the right cortex of the brain causing an ischemic stroke[17].

1.1.1. Induce anesthesia in the animal by using an inhalational mix of 5.0% isoflurane in 30% O_2/70% N_2.

1.1.2. Intubate the animal using a 20 GA catheter (Table of Materials) and connect to an automatic ventilator, set the flow rate based on the animal's body weight and keep the animal anesthetized using 1.5 – 2.0% isoflurane in 30% O_2/70% N_2.

1.1.3. Using a heating lamp and a rectal probe connected to a temperature controller device, keep the animal's body temperature at 37 °C.

1.1.4. Put a drop of lubricant eye ointment on the mouse's eyes.

1.1.5. Place the animal in a supine position and remove the hair from the neck area using a hair trimmer.

1.1.6. Clean the skin area by first using a cotton swab with povidone-iodine, and second using a sterile pad with 70% ethanol. Perform this thrice.

1.1.7. Verify the depth of anesthesia and the absence of pain by slightly pinching the animal's posterior paw.

1.1.8. Make a 0.8 cm sagittal incision on the middle line of the neck and expose the right CCA.

1.1.9. Prepare the suture for the CCA ligation by dissociating the 4–0 silk suture into the thinner threads that compose the main thread. Use 1.5 cm length of one of the subthreads to permanently ligate the CCA.

NOTE: After tightening the knot, remove the excess of thread by cutting the extension at 1–2 mm distance to the knot.

1.1.10. Apply a drop of bupivacaine before closing the wound.

1.1.11. Close the incision performing simple interrupted sutures using a 4–0 silk surgical suture and apply triple antibiotic ointment on the surface to prevent infections.

1.1.12. Move the mouse position to expose the right lateral side of the animal's body.

1.1.13. Make a 0.5 cm incision between the right eye and ear of the animal, exposing the joint between the skull and the temporal muscle.

1.1.14. Using a cautery loop, cauterize the muscle to separate it from the skull and expose the area of the MCA.

1.1.15. Drill a 0.2 mm^2 window to expose the MCA using an electric drill and stop the blood flow by electrocauterization.

NOTE: A single pulse at 80% power intensity is enough to cauterize the MCA.

1.1.16. Apply a drop of bupivacaine before closing the wound.

1.1.17. Close the incision performing simple interrupted sutures using a clear 4–0 nylon surgical suture and apply triple antibiotic ointment on the surface to prevent infections.

1.1.18. After completing the surgery, transfer the animal to an incubator with controlled temperature (32 °C) and allow the animal to recover.

1.1.19. After 2 h, transfer the animal to its home cage and provide food and water *ad libitum*.

1.2. Photothrombotic stroke (PT stroke).

NOTE: Briefly, PT stroke is performed by illuminating Rose Bengal within the vessels in the brain. Rose Bengal is administered intraperitoneally, and once it has been well distributed throughout the body (5 min), it is illuminated by a green cold light, which activates Rose Bengal to generate reactive oxygen species (ROS). These ROS damage the membrane of endothelial cells creating thrombi within the entire illuminated area and leading to local cerebral blood flow disruption[18].

1.2.1. Induce anesthesia in the animal by using an inhalational mix of 5.0% isoflurane in 30% O_2/70% N_2.

1.2.2. Set the animal to a stereotaxic frame keeping the animal anesthetized using a mask and 1.5 – 2.0% isoflurane in 30% O_2/70% N_2.

1.2.3. Keep the animal at 37 °C using a hot water recirculating heater and a rectal probe to measure that animal's body temperature.

1.2.4. Put a drop of lubricant eye ointment on the mouse's eyes.

1.2.5. Shave the animal's head using a hair trimmer.

1.2.6. Clean the shaved scalp area three times by using a cotton swab with povidone-iodine, and second using a sterile pad with 70% ethanol.

1.2.7. Verify the absence of pain by slightly pinching the animal's posterior paw.

1.2.8. Make a 1.4 cm sagittal incision on the middle line of the scalp using a scalpel and expose the skull.

1.2.9. Using a sharp pencil, make a mark at 1.5 mm from the bregma toward the right side.

1.2.10. Place a circular pinhole of 2.5 mm diameter centered on the 1.5 mm mark.

NOTE: A square containing a circular pinhole can be made by using double sided black tape and making a 2.5 mm diameter opening in the center by using a single-hole punch tool of the mentioned size.

1.2.11. Place the green cold light on the circular pinhole, keeping the gap between the light and the pinhole to a minimum.

1.2.12. Cover the area using aluminum foil to avoid the spread of the light.

1.2.13. Once the set-up is ready, inject the animal intraperitoneally with 10 mg/kg of Rose Bengal (10 mg/mL in 1x PBS) and wait for 5 min.

1.2.14. After 5 min, turn on the cold light source (intensity 4.25) and maintain the exposure for 15 min.

1.2.15. Next, turn off the cold light and verify the stroke either by naked-eye (the area is expected to be whiter than the surrounding area) or using external devices to measure the cerebral blood flow (for example, by using laser speckle contrast imaging (Table of Materials; see step 5.1).

1.2.16. Apply a drop of bupivacaine before closing the wound.

1.2.17. Close the incision performing simple interrupted sutures using a clear 4–0 nylon surgical suture and apply triple antibiotic ointment on the surface to prevent infections.

1.2.18. After completing the surgery, transfer the animal to an incubator with controlled temperature (32 °C) and allow the animal to recover.

1.2.19. After 2 h, transfer the animal to its home cage and provide food and water *ad libitum*.

2. Preparing PAUSAT for imaging

2.1. Turn on the 532 nm laser and leave it on for 15 min to warm-up.

2.2. Prepare the imaging platform for the anesthetized animal.

2.2.1. Place the customized ramp (Figure 2C) attached to the manually adjustable stage (Table of Materials) beside the imaging membrane.

2.2.2. Attach the mouse tooth-holder with the breathing tube connected to the customized ramp, and secure the heating pad on the surface of the ramp.

2.3. After the laser is warmed up, check that the laser path and coupling into the fiber-bundle is well-aligned using a near infrared detector card (Table of Materials) by placing the card in front of the fiber-bundle input and ensuring the laser light enters the bundle.

NOTE: Adjust any laser path mirrors as necessary to ensure the laser input is centered with the fiber-bundle input.

3. Preparing the animal for PAUSAT

NOTE: PAUSAT is performed 1 day following PT stroke surgery or 3 days following pMCAO surgery. Preparing PAUSAT for imaging (step 2) will take about 20 min and should be done immediately before preparing the animal for PAUSAT.

Induce anesthesia by briefly exposing the animal to 5% isoflurane mixed with 30% O_2/70% N_2 in a chamber.

3.1. Transfer the animal to a heated platform with a teeth-holder and a mask and maintain the anesthesia at 1.5 – 2.0 % isoflurane in 30 % O_2/70 % N_2.

3.2. Use a heating lamp and a rectal probe connected to a temperature controller device to keep the animal’s body temperature at 37 °C.

3.3. Trim the hair on the top of the animal's head by using an electric shaver. Include the region from near the eyes to behind the ears.

3.4. Shave the hair on the top of the animal's head by applying a commercial hair removal cream to completely remove the remaining short hair. Leave on the skin for 5 – 6 min, then wipe off using a cotton swab dabbed in water to help fully remove the cream. Repeat until the skin is clear of hair.

3.5. Once the animal and the system are ready for imaging, and right before transferring the animal to the system's platform, inject a 100 μL solution of microbubbles at the stock concentration (Table of Materials) retro-orbitally using a 27 G needle.

NOTE: Once the bubbles are in circulation in the bloodstream, there is a limited amount of time to image without a significant loss of signal (~10 min).

3.6. Put a drop of eye protection lotion on the mouse's eyes.

4. PAUSAT Imaging

NOTE: This is done to image the contra- and ipsi-lateral regions of the brain after stroke

4.1. Transfer the mouse to the integrated PAUSAT (Table of Materials) image platform, placing the mouse in a supine position on the customized ramp (Figure 2C).

4.2. Fill the imaging window with enough distilled water on the surface for acoustic coupling.

NOTE: An optional ramp –printed using a 3D printer- is recommended to prevent the animal's body from getting wet during the image acquisition and improve the animal's comfort. It also helps maintain a stable body temperature. Furthermore, the ramp can be attached to a manual stage (Table of Materials) to adjust the focal depth of the dual-element wobbler transducer relative to the mouse head. The custom ramp design file is available upon request to the authors.

4.3. Secure the mouse head in the tooth-holder and ensure the proper anesthesia and air flow.

4.4. Using a heating lamp and a rectal probe connected to a temperature controller device, keep the animal's body temperature at 37 °C.

4.5. Open the imaging application (Table of Materials) and navigate to B-mode ultrasound.

4.6. Use the live ultrasound window to manually adjust the mouse head to the desired position.

4.7. Use the live ultrasound window to adjust the height of the stage such that the focal depth of the transducer (19 mm) is approximately in the middle of the area to be imaged.

4.8. Image with B-mode ultrasound.

4.8.1. Adjust the value of the ultrasound transmit frequency in B-mode (for these studies, use 16 MHz).

4.8.2. Input the save directory information in the imaging application.

4.8.3. Use the floating box to select the desired region for the B-mode scan of the brain.

4.8.4. Press the “Acquire Static” button.

4.8.5. Check the results of the scan in the application once the image acquisition is completed to ensure that the desired region was imaged.

NOTE: Avoid unnecessary delays in the B-mode imaging acquisition to ensure that a high enough concentration of microbubbles remains in the bloodstream for the acoustic angiography.

4.9. Image with acoustic angiography.

4.9.1. Return to “Image Acquisition”.

4.9.2. Change to “Acoustic Angiography” mode in the imaging application (Table of Materials).

4.9.3. Input the desired scan protocol parameters (most important of which is the frame spacing and the number of frames per position, which was set to 0.2 mm and 10, respectively for these studies).

4.9.4. Press the “Acquire Static” button.

NOTE: The acoustic angiography acquisition will take longer than the B-mode ultrasound.

4.9.5. Once the scan is completed, check the results of the scan under “Image Analysis” to ensure that the image quality is as expected.

NOTE: For AA mode, a more representative whole-brain volume can be acquired by repeating a second scan at a different focal depth inside the brain and later recombining the images with proper post-processing (see Figure 3).

4.10. Image with photoacoustic tomography.

4.10.1. Open the optical parametric oscillator (OPO) application (Table of Materials) and set it to 756 nm.

NOTE: OPOs can get easily out of calibration, so prior to the experiment ensure that the OPO is calibrated correctly by using an independent spectrometer.

4.10.2. Manually translate the linear-array transducer to the previously determined coordinates to ensure that the wobbler volumes and the linear-array volumes are automatically co-registered.

NOTE: It is critical that a co-registration experiment using a phantom grid is done beforehand to determine the exact distance needed to translate the stage such that the resulting data from both transducers are co-registered in 3D.

4.10.3. Open the laser application and turn on the 532 nm laser.

4.10.4. Using a laser power meter, measure the energy of the laser output and ensure it is the desired energy (~10 mJ per pulse were used for these studies).

4.10.5. Select the desired scanning parameters for PAT (0.4 mm step size, 20 mm scan length, and 10 frames averaged per position).

4.10.6. Open the ultrasound data acquisition system MATLAB program (Table of Materials) and press the “Run” button.

4.10.7. Acquire the PAT scan by pressing the “Start” button.

4.10.8. Once the scan is complete, open the MATLAB save program. Change the save name to the desired file name and press the “Run” button.

4.10.9. Change the OPO wavelength to 798 nm and repeat the steps from 4.10.3 to 4.10.8.

NOTE: For a longitudinal study, it would be recommended to allow the animal to recover by placing it in an incubator and under observation for a few hours until the animal recovers (following steps 1.1.18 and 1.1.19). If result validation is desired, continue to step 5 immediately after PAUSAT imaging.

5. Optional: Results validation

5.1. Laser speckle contrast imaging (LSCI).

5.1.1. Anesthetize the animal using 1.5 – 2.0% isoflurane in 30 % O_2/70% N_2.

5.1.2. Set the animal to a stereotaxic frame keeping the animal anesthetized using a mask and the above-mentioned inhalational anesthesia.

5.1.3. Keep the animal at 37 °C using a hot water recirculating heater and a rectal probe to measure the animal’s body temperature.

5.1.4. Put a drop of eye protection lotion on the mouse’s eyes.

5.1.5. Verify the absence of pain by slightly pinching the animal’s posterior paw.

5.1.6. Make a 1.4 mm sagittal incision on the middle line of the scalp and expose the skull. Use forceps to hold the scalp and prevent it from occupying the area of the brain to scan.

5.1.7. Apply some drops of saline on the skull and place the laser speckle contrast system device (Table of Materials) over the animal’s head.

5.1.8. Press the “File” menu and set the device in “Online mode” contained in the submenu “Working Mode”.

5.1.9. Select the default image storage folder in the “File” menu, and the submenu “Save Settings”.

5.1.10. In the “Light Source” menu, connect the guiding laser (“Laser on”) and the white light (“White-light on”) to locate the imaging window at the right position.

5.1.11. In the “Setting menu”, select “Magnification settings”, move the cursor manually to 2.5 and press “Apply” and “OK” to save the settings.

5.1.12. Adjust the focus by manually moving the focus bar located in the top submenu of the main page.

5.1.13. In the “Setting menu”, select “Pseudo Color Threshold Setting”, adjust the threshold as desired, press “Apply”, then “OK” to save the settings.

5.1.14. In the “Light Source” menu, disconnect the guiding laser (“Laser off”) and the white light (“White-light off”) before capturing the image.

5.1.15. Capture the image by selecting the “Play” symbol in the top submenu of the main page.

5.2. Triphenyltetrazolium chloride (TTC) staining.

5.2.1. Deeply anesthetize the animal using 5% isoflurane in 30% O_2/70% N_2.

5.2.2. Once the animal has stopped breathing, decapitate it using big scissors.

5.2.3. Remove all the skin around the head and the muscles in the neck area.

5.2.4. Make a sagittal cut in the occipital part of the skull until it reaches the parietal bone.

5.2.5. Make a horizontal cut (~ 5 mm) in the left and right side below the blood vessel. Remove the occipital bone of the skull using straight forceps.

5.2.6. Make a cut (~ 5 mm) at the frontonasal suture of the skull.

5.2.7. Make a sagittal cut (~ 10–15 mm) in the midline of the skull – between hemispheres - and make sure they are completely separated.

5.2.8. Using Size #7 curved scissors, remove the parietal left and right bones of the skull from the center to the sides.

5.2.9. Transfer the brain to a container filled with 5 mL of ice-cold PBS 1x and keep it on ice for 10 min.

5.2.10. Transfer the brain to a stainless-steel brain matrix (1 mm thickness sections).

5.2.11. Section the brain in 1 mm coronal sections using disposable razor blades (Table of Materials).

5.2.12. Holding the blades by their sides, transfer into a container filled with ice-cold 1x PBS.

5.2.13. Carefully separate the sections from the blades one by one.

5.2.14. Transfer the brain slices into a 70 μm diameter Petri dish containing 5 mL of 2% TTC (Table of Materials, 3) in 1x PBS.

5.2.15. Incubate for 15 min in the dark at room temperature (R/T).

5.2.16. After 15 min, discard the TTC and replace it with 3 mL of formalin and incubate in the dark for at least 30 min at R/T.

5.2.17. Finally, transfer the brain slices onto a transparent plastic and scan the samples including a ruler in the scan image as a reference for future measurements.

REPRESENTATIVE RESULTS:

Imaging of blood vessel morphology in the brain

AA generates blood vessel morphology images by exciting microbubbles in the circulatory system at their resonant frequency and receiving the super harmonic response of the microbubbles. By using the customized ramp (Figure 2C) attached to a manually adjustable stage, we can image the mouse brain with AA mode at two different focal depths. When deeper regions are targeted, more superficial regions (such as the cerebral cortex) show a poorer resolution and signal strength (Figure 3A), and vice versa (Figure 3B). However, by acquiring two focal depths and combining them, AA images can provide information about a whole coronal section (Figure 3C, D). Additionally, by using the motorized stage to scan along a third dimension, PAUSAT can register a series of coronal images covering the region of interest (ROI) defined by the user. These series of images can be aligned and used to visualize a 3D representation of the whole brain, or the ROI defined by the user. However, additional results demonstrating that other quantitative measures (such as the stroke volume) can be analyzed by using the 3D information from the compilation of images acquired by PAUSAT will also be provided here.

Anatomical and functional evaluation before and after ischemic stroke

To illustrate the potential of the PAUSAT system in preclinical studies, we studied two groups of animals subjected to one of the models of ischemic stroke analyzed here: pMCAO or PT stroke. These two stroke models differ in the principles by which the ischemic region is created. Briefly, in the pMCAO model the middle cerebral artery is electro-cauterized stopping the blood supply from this artery to the brain. This injury triggers a secondary injury in which surrounding tissue becomes ischemic, enlarging the area affected by the stroke. We decided to image the pMCAO stroke brain at day three after the stroke, because this is the time at which the maximum area expected to be affected by the stroke is achieved. In the PT stroke, however, the maximum area of tissue affected by the stroke is achieved after the first day, so we decided to image PT stroke at day one after the stroke was performed. Although we chose these timepoints in our study, PAUSAT can be used for longitudinal monitoring of stroke at any desired timepoint.

First, a B-mode scan was acquired to ensure the right position of the animal’s head and identify the spatial limits between the skull and the brain (Figures 4A and 5A). The most anterior part of the brain imaged includes the frontonasal suture of the skull as a reference point. An ROI of 20 (anterior to posterior) x 17.15 (lateral) mm covering the left (contralateral, CL) and the right (ipsilateral, IL) hemispheres was defined in the following studies to locate the stroke region. AA images provide information regarding the blood vessels structures by targeting the signal from the circulating microbubbles. Our results

show that in the uninjured brain (baseline), both hemispheres present a similar distribution of blood vessels (Figures 4B and 5B), as expected in the absence of injury. A similar result is observed for the tissue oxygenation map distribution based on PA images obtained at two different wavelengths (Figures 4C and 5C). We decided to evaluate two different wavelengths based on the local maximum optical absorption for deoxygenated hemoglobin (756 nm) and the wavelength at which the deoxygenated and oxygenated hemoglobin present equal optical absorption (798 nm)[19]. By capturing these two states of hemoglobin we can accurately estimate tissue oxygenation (Figures 4D and 5D).

The day after acquiring the baseline image from the brain, we performed surgery on the animal (pMCAO or PT stroke) as described in previous sections. A new set of images were acquired at a specific timepoint after the stroke (see Figure 2A) to evaluate the location and size of the stroke. The AA images acquired from mice subjected to pMCAO show a notable reduction in the intensity of the signal in the right lateral of the cortex (Figure 4B). The same region shows a reduction in the tissue oxygenation map from PA images, suggesting an ischemic area (Figure 4D). To validate our results, we decided to harvest the brain and perform a TTC staining immediately after acquiring the images from the stroke animal. Our results show that the area identified as stroke is similar when compared with our results by PAUSAT and the well-established TTC staining (Figure 4B–E). We also demonstrate here that PAUSAT can identify stroke areas in the brain using a second model of stroke, PT stroke, evaluated at an earlier time point after the stroke induction (1 day). As shown in Figure 5B, we were able to identify a region in the upper part of the cortex with a reduced blood flow supply and a concomitant decrease in oxygen saturation (Figure 5D). The results obtained from TTC staining match the location and size of the stroke previously identified by PAUSAT (Figure 5 B–E).

The age of the mouse being imaged can heavily affect the image quality. The skull of a mouse becomes thicker with age, and since the skull has a significantly different acoustic impedance relative to soft tissue, a large percentage of the ultrasonic waves are reflected at the skull boundary. Because these integrated imaging systems are all acoustic based, this leads to a decrease in imaging depth for older mice. This can be clearly seen in Figure 6, where mice of three different ages were imaged with AA under the same conditions. Similar low signal results are expected if the imaging procedure is not followed as previously described.

Quantitative analysis of the stroke volume by PAUSAT

As described in the above-mentioned results, PAUSAT captures a series of coronal images targeting an ROI described by the user. We analyzed the volume of stroke by calculating the stroke area within the different coronal images and the distance between images. The stroke volume calculated by PAUSAT shows no statistical difference ($p < 0.05$) compared to the stroke volume calculated based on a similar approach using TTC staining images (Figure 7).

DISCUSSION:

There are a few vital aspects of this method that, if done incorrectly, can lead to significantly decreased image quality and quantitative analysis. The most commonly occurring result of

user-error in PAUSAT images is either a lack of signal or very low signal strength, both of which can occur for a variety of reasons. One such reason is a problem with the acoustic coupling. Large air bubbles in the water surrounding the mouse's head during imaging can often block ultrasound from travelling to or from the transducer. This will cause a shadow region in the resulting image for all three modalities of the system. This can be prevented by ensuring that enough water is present between the system membrane and the sample to be imaged. It could also happen that there is a lack of AA signal, but a surprisingly high PA signal, independent of the wavelengths used. This could be due to the presence of hair –especially dark hair- interfering with the absorption of the light. To avoid this, it is necessary to have previously shaved the animal's head until no hair is visually identifiable.

Regarding AA images, another problem that might occur and would lead to the lack of or very low signal is a low concentration of microbubbles present in the circulatory system. If the microbubbles are too diluted or they were injected improperly, the resulting signal will be very weak. Note that the retro-orbital injection must be performed only by a well-trained personnel. Another reason is that a long time passed between the microbubble injection and the start of imaging, which can lead to a reduction of the microbubbles in the bloodstream. To avoid this, it is recommended to prepare the system for imaging before injecting the microbubbles, so the animal can be transferred to the PAUSAT system membrane immediately after injection. It is worth mentioning that alternative intravenous routes (such as tail vein injection) can also be used once the animal is already positioned on the PAUSAT system membrane, shortening the time between injection and imaging. Additionally, in the interest of maintaining the maximum concentration of microbubbles possible, it is also recommended to perform the AA imaging before the PA imaging.

PA signal can also be affected if the necessary steps are not properly performed. One of the issues involves the quality of the excitation laser. The two main components that describe the laser source are the pulse energy and the wavelength. It is highly recommended to use an independent power meter and spectrometer to measure these quantities and ensure they are set to the desired values. If an incorrect value is assumed, the functional calculations will provide misleading results.

It is also possible that when AA and PA images are combined, they are out of alignment. The main reason is that the coordinates established between transducers were not accurate. To prevent this, it is critical to perform the required experiments using a phantom grid beforehand to determine the exact coordinates for a successful co-registration of AA and PA images. Another potential source of inaccuracy is due to incorrect calibration of the OPO. To mitigate this, the OPO must be correctly calibrated using an independent spectrometer.

There remain significant areas of improvement, particularly regarding the image quality of the PAT component of this integrated system. The current PAT system is based on a scanning linear-array configuration. We are able to observe large-scale differences in oxygenation of infarct versus healthy regions of the brain using several stroke mouse models, however the detailed vasculature (microvessels) is not able to be seen. There are two main problems that contribute to this low image quality. The first is the limited-view problem. In order to create a full-view reconstructed image of a sample in PAT, the detector must completely

surround the object (or have a solid angle of 4π). However, in the experimental setting this is difficult. This gives rise to the limited view problem, leading to blood vessels that are orthogonal to the transducer array being undetectable[20]. Solutions to reduce the effects of the limited-view problem in linear-array PAT do exist, the most promising of which is the use of microbubbles as virtual point sources[21]. The second problem of linear-array PAT is poor elevational resolution and sensitivity due to the weak focus of the acoustic lens. However, the use of single-slit diffraction in the hardware design of a linear-array system has been shown to create isotropic resolution and sensitivity for linear-array PAT[22,23]. Deep learning approaches have also been shown to partially resolve both the limited-view problem and the poor elevational resolution of linear-array PAT[24–26]. The combination of these solutions would significantly enhance the image quality of the PAT component of our integrated imaging system.

Here, we have presented a novel non-invasive multi-modal imaging method for the structural and functional quantification of ischemic stroke in the preclinical setting. Through AA, clear morphology and perfusion mapping of blood vessels in the mouse brain is possible. A locally defined lack of signal can indicate an infarct region where there is decreased blood perfusion, allowing for the estimation of infarct volume noninvasively and longitudinally. Through PAT, the oxygen saturation of hemoglobin can be measured in and outside of the stroke region, showing the hypoxic state of brain tissues in the infarct region. This method of whole-brain imaging is low-cost with respect to some alternatives, such as small-animal MRI. Furthermore, it allows for the combination of functional and structural information in deep tissue that other preclinical imaging devices are unable to achieve. Compared to histological analyses, this method allows for measurement of these metrics longitudinally and at multiple timepoints, as opposed to at a single endpoint. The ability to do so will provide unprecedented quantitative detail in the preclinical study of ischemic stroke. Additionally, the structural and functional imaging capability of this system can be applied to many preclinical studies beyond ischemic stroke[27]. Any disease state or biological phenomenon affecting the vascular system could be studied in depth using PAUSAT, making it a powerful preclinical imaging tool translatable to many other preclinical fields (e.g., cancer).

ACKNOWLEDGMENTS:

The authors would like to acknowledge the engineering team at SonoVol Inc. for their technical support. This work was partially sponsored by American Heart Association Collaborative Sciences Award (18CSA34080277), to J. Yao and W. Yang; The United States National Institutes of Health (NIH) grants R21EB027981, R21 EB027304, RF1 NS115581 (BRAIN Initiative), R01 NS111039, R01 EB028143; The United States National Science Foundation (NSF) CAREER award 2144788; and Chan Zuckerberg Initiative Grant (2020–226178), to J. Yao; The NIH grants R21NS127163 and R01NS099590 to W. Yang.

REFERENCES:

1. Durukan A & Tatlisumak T Acute ischemic stroke: overview of major experimental rodent models, pathophysiology, and therapy of focal cerebral ischemia. Pharmacology Biochemistry and Behavior 87 (1), 179–197 (2007). [PubMed: 17521716]
2. Van der Worp HB & van Gijn J Acute ischemic stroke. New England Journal of Medicine 357 (6), 572–579 (2007). [PubMed: 17687132]

3. Hochrainer K & Yang W Stroke proteomics: from discovery to diagnostic and therapeutic applications. Circulation Research 130 (8), 1145–1166 (2022). [PubMed: 35420912]
4. Wang LV & Yao J A practical guide to photoacoustic tomography in the life sciences. Nature methods 13 (8), 627–638 (2016). [PubMed: 27467726]
5. Aldrich JE Basic physics of ultrasound imaging. Critical care medicine 35 (5), S131–S137 (2007). [PubMed: 17446771]
6. Jacques SL Optical properties of biological tissues: a review. Physics in Medicine & Biology 58 (11), R37 (2013). [PubMed: 23666068]
7. Li M, Tang Y & Yao J Photoacoustic tomography of blood oxygenation: a mini review. Photoacoustics 10 65–73 (2018). [PubMed: 29988848]
8. Menozzi L, Yang W, Feng W & Yao J Sound out the impaired perfusion: Photoacoustic imaging in preclinical ischemic stroke. Frontiers in Neuroscience (2022).
9. Gessner RC, Frederick CB, Foster FS & Dayton PA Acoustic angiography: a new imaging modality for assessing microvasculature architecture. International journal of biomedical imaging 2013 (2013).
10. Dayton PA & Rychak JJ Molecular ultrasound imaging using microbubble contrast agents. Frontiers in Bioscience-Landmark 12 (13), 5124–5142 (2007).
11. Isayama K, Pitts LH & Nishimura MC Evaluation of 2, 3, 5-triphenyltetrazolium chloride staining to delineate rat brain infarcts. Stroke 22 (11), 1394–1398 (1991). [PubMed: 1721247]
12. Ruan J & Yao Y Behavioral tests in rodent models of stroke. Brain Hemorrhages 1 (4), 171–184 (2020). [PubMed: 34322665]
13. Parthasarathy AB, Kazmi SS & Dunn AK Quantitative imaging of ischemic stroke through thinned skull in mice with Multi Exposure Speckle Imaging. Biomedical optics express 1 (1), 246–259 (2010). [PubMed: 21258462]
14. Hingot V et al. Early Ultrafast Ultrasound Imaging of Cerebral Perfusion correlates with Ischemic Stroke outcomes and responses to treatment in Mice. Theranostics 10 (17), 7480 (2020). [PubMed: 32685000]
15. Menozzi L et al. Three-dimensional non-invasive brain imaging of ischemic stroke by integrated photoacoustic, ultrasound and angiographic tomography (PAUSAT). Photoacoustics 100444 (2022).
16. Llovera G, Roth S, Plesnila N, Veltkamp R & Liesz A Modeling stroke in mice: permanent coagulation of the distal middle cerebral artery. JoVE (Journal of Visualized Experiments) (89), e51729 (2014). [PubMed: 25145316]
17. Trotman-Lucas M, Kelly ME, Janus J, Fern R & Gibson CL An alternative surgical approach reduces variability following filament induction of experimental stroke in mice. Disease Models & Mechanisms 10 (7), 931–938 (2017). [PubMed: 28550100]
18. Labat-Gest V & Tomasi S Photothrombotic ischemia: a minimally invasive and reproducible photochemical cortical lesion model for mouse stroke studies. JoVE (Journal of Visualized Experiments) (76), e50370 (2013).
19. Matsumoto Y et al. Visualising peripheral arterioles and venules through high-resolution and large-area photoacoustic imaging. Scientific reports 8 (1), 1–11 (2018). [PubMed: 29311619]
20. Xu Y, Wang LV, Ambartsoumian G & Kuchment P Reconstructions in limited-view thermoacoustic tomography. Medical physics 31 (4), 724–733 (2004). [PubMed: 15124989]
21. Tang Y et al. High-fidelity Deep Functional Photoacoustic Tomography Enhanced by Virtual Point Sources. Photoacoustics 100450 (2023).
22. Zheng W, Huang C, Zhang H & Xia J Slit-based photoacoustic tomography with co-planar light illumination and acoustic detection for high-resolution vascular imaging in human using a linear transducer array. Biomedical Engineering Letters 1–9 (2022).
23. Wang Y et al. Slit-enabled linear-array photoacoustic tomography with near isotropic spatial resolution in three dimensions. Optics letters 41 (1), 127–130 (2016). [PubMed: 26696175]
24. Vu T, Li M, Humayun H, Zhou Y & Yao J A generative adversarial network for artifact removal in photoacoustic computed tomography with a linear-array transducer. Experimental Biology and Medicine 245 (7), 597–605 (2020). [PubMed: 32208974]

25. Zhang H et al. Deep-E: A fully-dense neural network for improving the elevation resolution in linear-array-based photoacoustic tomography. IEEE Transactions on Medical Imaging 41 (5), 1279–1288 (2021).

26. Hauptmann A et al. Model-based learning for accelerated, limited-view 3-D photoacoustic tomography. IEEE transactions on medical imaging 37 (6), 1382–1393 (2018). [PubMed: 29870367]

27. Li M et al. Three-dimensional Deep-tissue Functional and Molecular Imaging by Integrated Photoacoustic, Ultrasound, and Angiographic Tomography (PAUSAT). IEEE Transactions on Medical Imaging (2022).

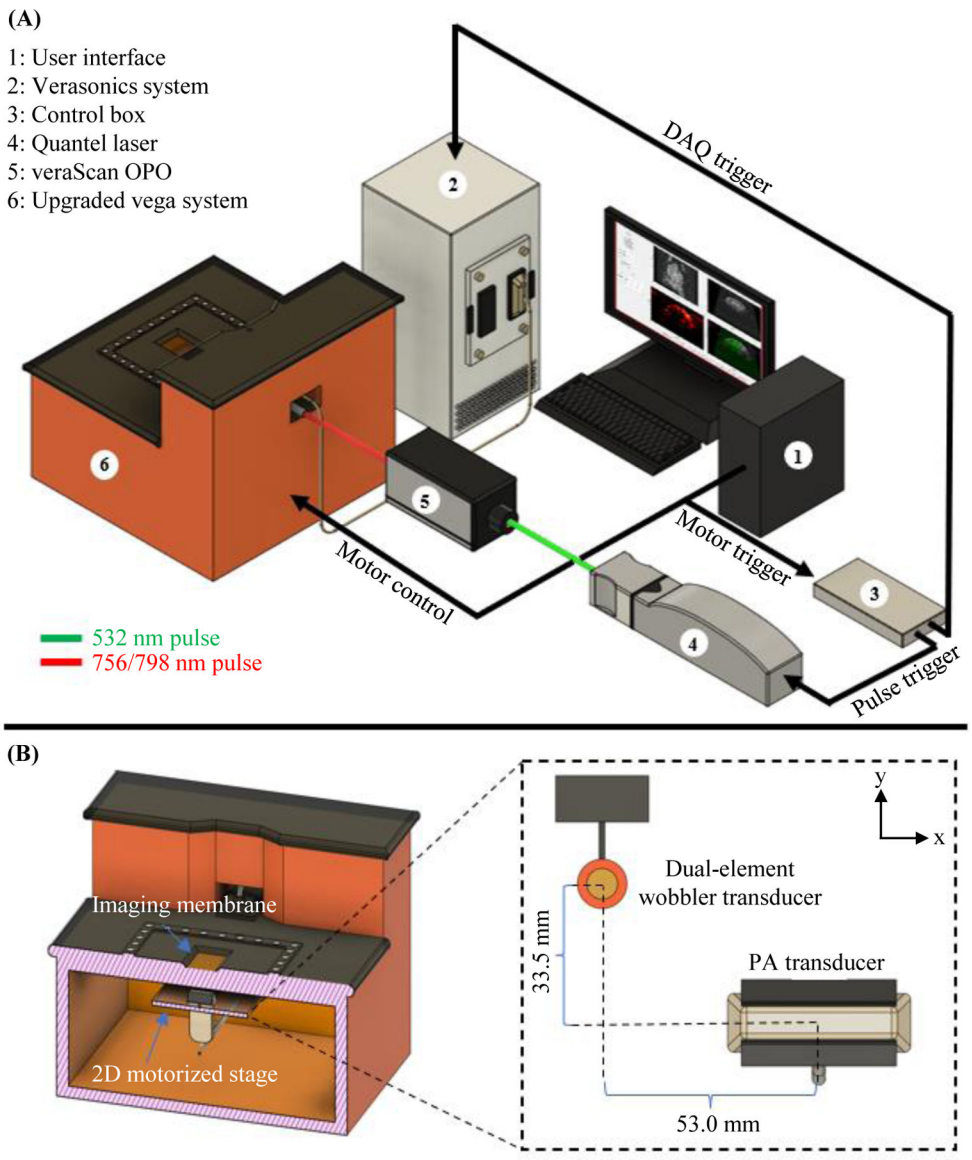

Figure 1: PAUSAT diagram.

(A) Complete schematic of the PAUSAT system, including the laser and optical parametric oscillator (OPO) used for PAT. (B) Inside view of PAUSAT system, including two ultrasound transducers. The dual-element wobbler transducer is used for both B-mode ultrasound and AA, and the linear-array transducer is used for PAT. Both transducers are mounted on the same 2D motorized stage, allowing for scanning to generate volumetric data. This figure has been modified from reference 15.

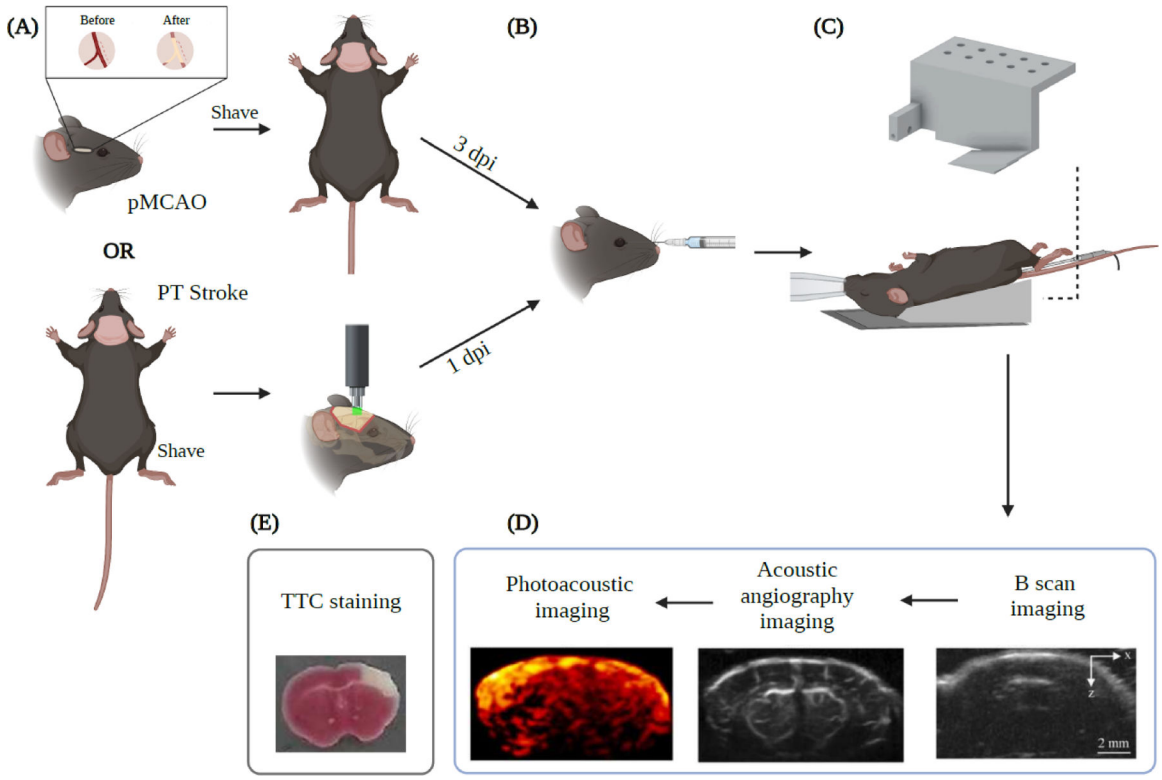

Figure 2: Summary of experimental procedure for PAUSAT imaging applied to stroke

The figure shows the workflow of the imaging procedure starting from (A) the two main stroke models (pMCAO and PT stroke). (B) A retro-orbital injection of the microbubbles must be performed prior to positioning the animal on the PAUSAT membrane. (C) A mask providing continuous anesthesia and a heating pad to keep the animal's body temperature stable are required in this setup. The animal's body is placed on the heating pad while the head rests on the membrane of the system. (D) The order of image acquisition is also displayed in the figure. (E) TTC staining is performed to validate our results in this study. DPI: days post injury.

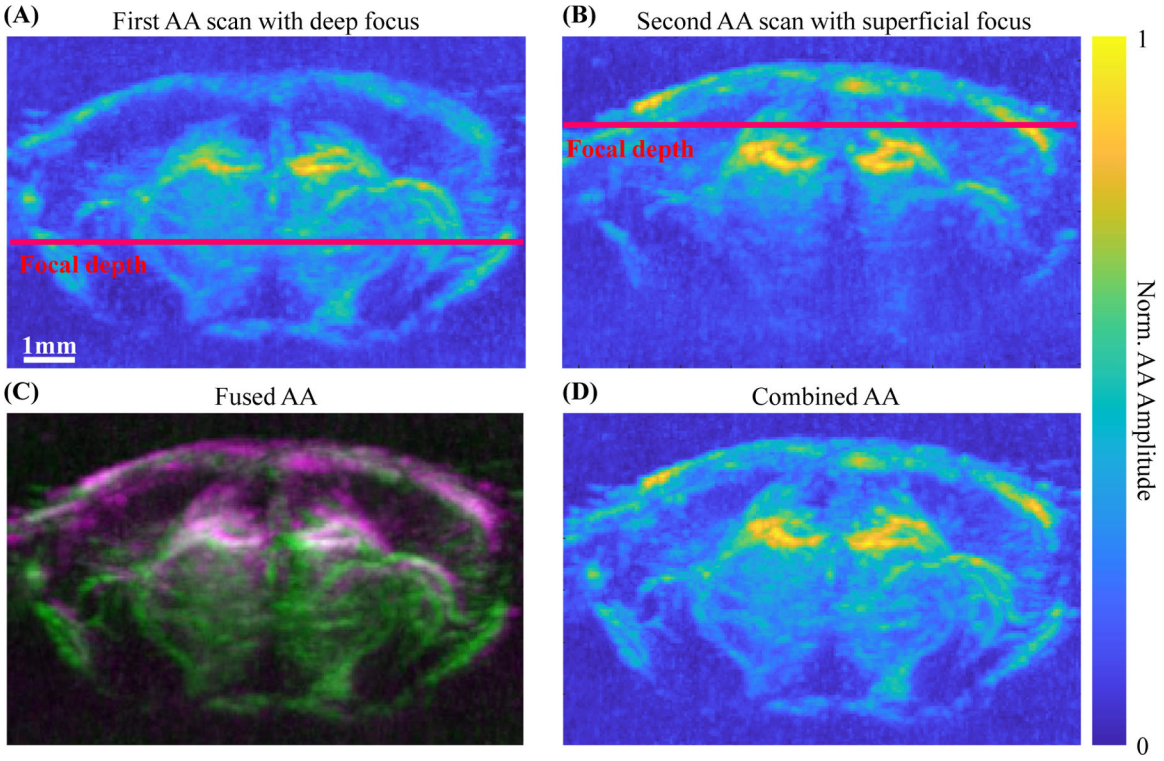

Figure 3: Effect of focal depth of wobbler transducer on the quality of AA images.

Images at multiple focal depths can be acquired and later combined to produce the best whole-brain imaging results. (A) AA coronal section acquired at a deeper focal depth. (B) AA coronal section acquired at more superficial focal depth. (C) Result of fusing deeper focus (green) and more superficially focused (magenta) images. (D) Result of combining deeper focus and more superficially focused images with a pixel scale value comparable to (A) and (B). This figure has been modified from reference 15.

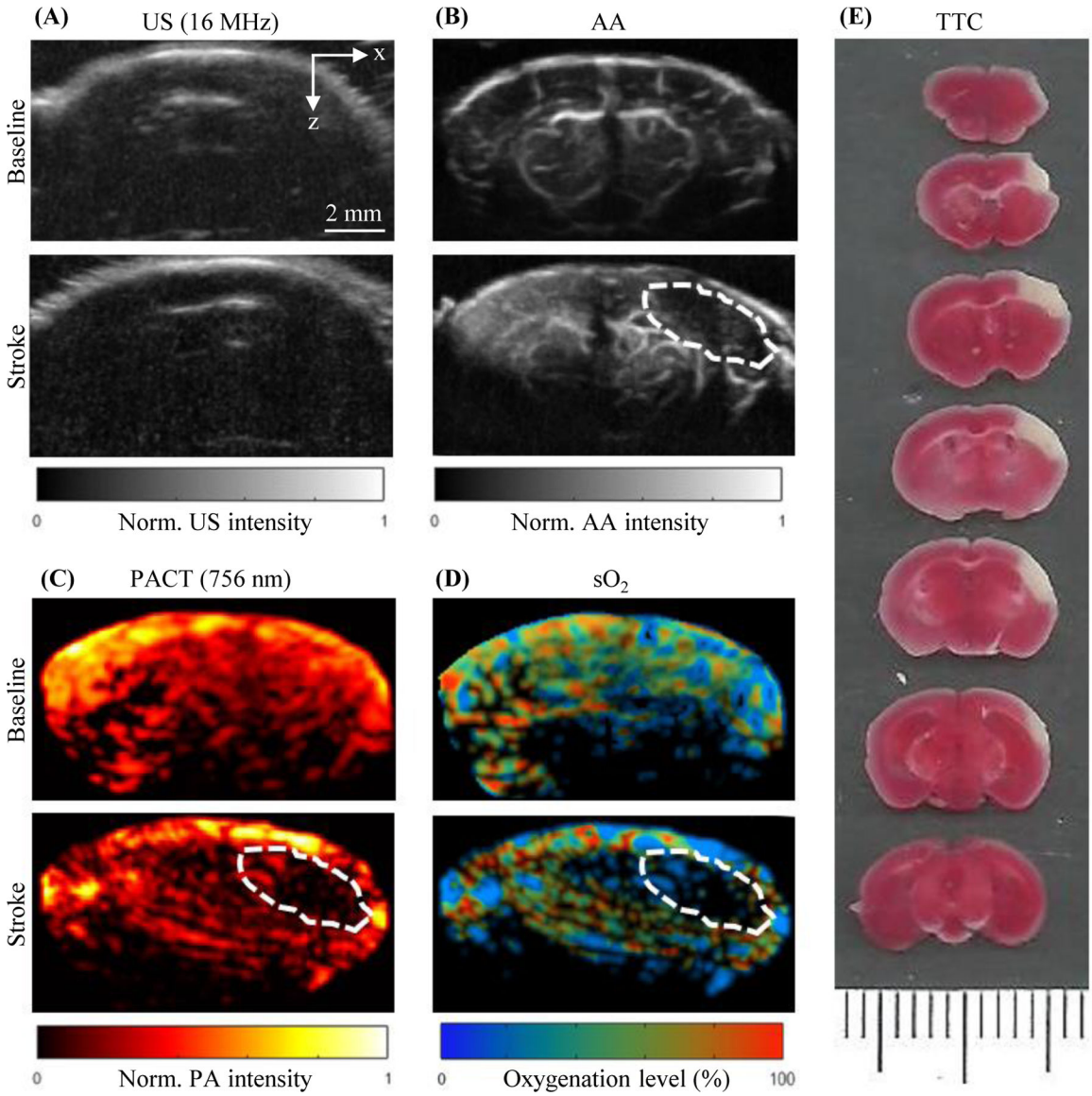

Figure 4: Representative PAUSAT results of a mouse brain before and after pMCAO stroke.
(A) Baseline and post-stroke B-mode ultrasound coronal images. (B) Baseline and post-stroke AA coronal images. (C) Baseline and post-stroke PA coronal images at 756 nm excitation. (D) Oxygen saturation map based on 756 nm and 798 nm excitation images. (E) TTC stained sections of mouse brain, showing the same region of stroke. The distance between the lines on the bottom of the image represents 1 mm. This figure has been modified from reference 15.

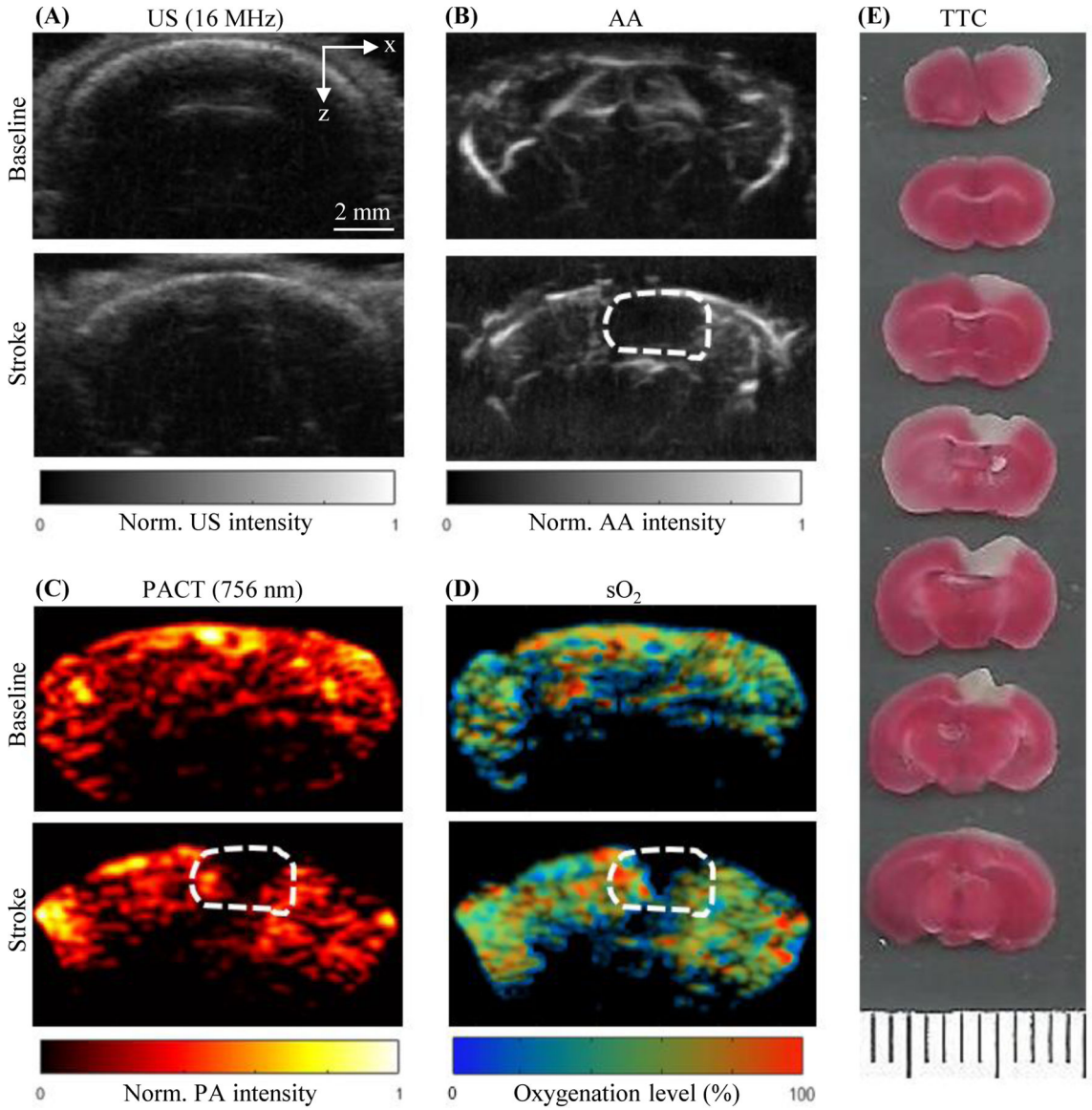

Figure 5: Representative PAUSAT results of a mouse before and after PT stroke.

(A) Baseline and post-stroke B-mode ultrasound coronal images. (B) Baseline and post-stroke AA coronal images. (C) Baseline and post-stroke PA coronal images at 756 nm excitation. (D) Oxygen saturation map based on 756 nm and 798 nm excitation images. (E) TTC stained sections of mouse brain, showing the same region of stroke. The distance between the lines on the bottom of the image represents 1 mm. This figure has been modified from reference 15.

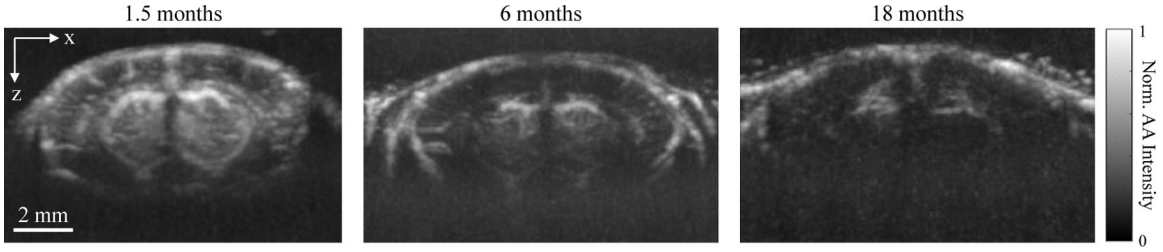

Figure 6: Effect of mouse age on the quality of AA images.

This figure shows the difference in AA signal intensity and imaging depth when animals from different ages are imaged under comparable conditions. As seen in the figure, older mice (18 months) imaging produces lower quality images due to the size and thickness of the skull compared to younger mice (1.5 months), while adult mice show an intermediate signal (6 months). Due to the large acoustic impedance mismatch between the skull and brain tissue, ultrasound waves propagating through the skull are reflected and refracted, leading to signal loss and resolution degradation.

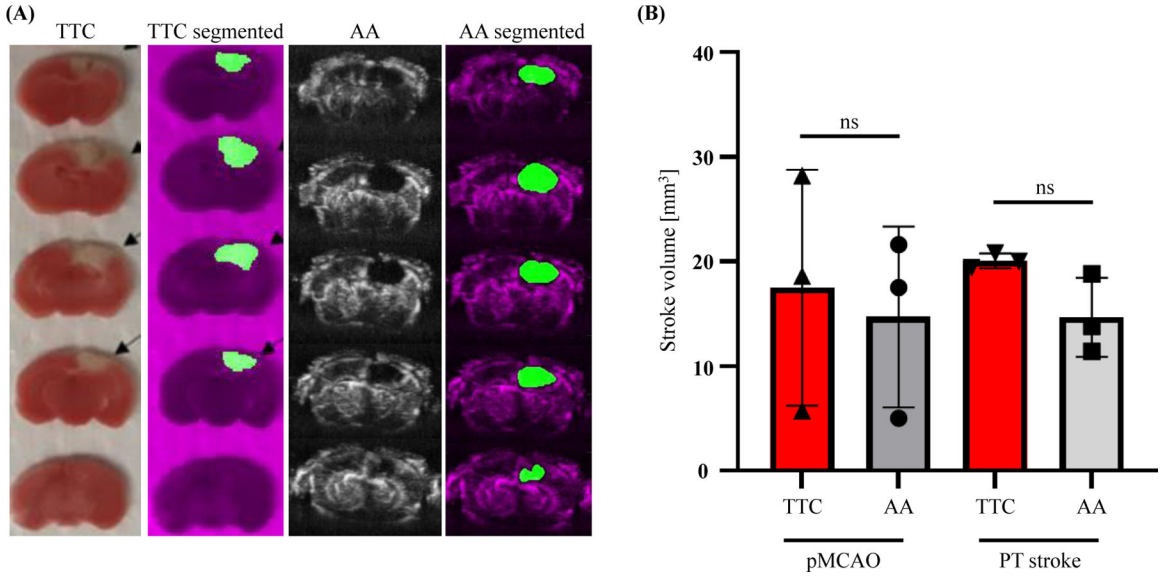

Figure 7: Analysis of the volume of the ischemic stroke.

(A) Example of TTC sections from PT stroke and corresponding TTC segmented images, AA images, and AA segmented images at comparable coronal locations. (B) Shows the stroke volume calculated based on TTC and AA images for pMCAO and PT stroke showing no significant differences ($p > 0.05$). The graph shows the mean ± standard deviation (S.D.) (n=3 animals per group). This figure has been modified from reference 15.

MATERIALS:

Name of Material/ Equipment	Company	Catalog Number	Comments/Description
20 GA catheter	BD Insyte Autoguard Winged	381534	For mouse intubation
2,3,5-Triphenyltetrazolium chloride	Sigma	T8877	Necessary for TTC-staining brain for validation
532nm Laser	Quantel	Q-smart 850	Laser used to pump the OPO for PAT
Automatic Ventilator Rovent Jr.	Kent Scientific	RV-JR	To keep mice under anesthesia during surgical procedure
Black braided silk 4–0 USP	Surgical Specialties	SP116	Used for sutures on the neck for pMCAO surgery
Bupivacaine	Hospira	0409-1159-18	Used prior to closing wounds during surgical procedure
C57BL/6 Mice	Jackson Lab	#000664	Mice used for studying ischemic stroke (2–6 month old male/female)
Clear suture	Ethicon	8606	Used for closing wound (PT stroke and pMCAO). A clear suture won't interfere with PAT
Cold Light LED	Schott	KL 1600	Needed to create PT stroke
Disposable Razor Blade	Accutec Blades	74–0002	For sectioning mouse brain
Electric drill	JSDA	JD-700	Used to expose MCA during pMCAO procedure
Electrocauterization tool	Wet-Field	Wet-Field Bipolar-RG	Stops blood flow after drilling during pMCAO procedure
Hair removal gel	Veet	8282651	Used to remove hair from mouse prior to imaging
High Temperature Cautery Loop Tip	BOVIE Medical Corporation	REF AA03	Used to avoid bleeding when separating the temporal muscle from the skull
IR Detector Card	Thorlabs	VRC5	Used to ensure light path is aligned
Laser Power Meter	Ophir	StarBright, P/N 7Z01580	Can be used to calibrate the laser energy prior to imaging
Laser Speckle Imaging System	RWD Life Science Co.	RFLSI-III	Can be used to validate stroke surgery success
Lubricant Eye Ointment	Soothe	AB31336	Can be used to avoid drying of the eyes
Manually adjustable stage	Thorlabs	L490	Used with custom ramp for multiple focal depth AA imaging
Modified Vega Imaging System	Perkin Elmer	LLA00061	System containing both B-mode/AA and PAT transducers
Optical Parametric Oscillator	Quantel	versaScan-L532	Allows for tuning of excitation wavelength in a large range
Programmable Ultrasound System	Verasonics	Vantage 256	Used for PAT part of system
Rose Bengal	Sigma	330000	Necessary to induce PT stroke
Suture	LOOK	SP116	Used for permanent ligation of CCA
Temperature Controller	Physitemp	TCAT-2	Used to maintain stable body temperature of mice during procedures
VesselVue Microbubbles	Perkin Elmer	P-4007001	Used for acoustic angiography (2.43 × 10^9 microbubbles/mL)